How β-skeletons lose their edges

Q1 Andrew Adamatzky

University of the West of England, Bristol, United Kingdom

ABSTRACT

A β-skeleton is a proximity graphs with node neighbourhood defined by continuous-valued parameter β. Two nodes in a β-skeleton are connected by an edge if their lune-based neighbourhood contains no other nodes. With increase of β some edges a skeleton are disappear. We study how a number of edges in β-skeleton depends on β. We speculate how this dependence can be used to discriminate between random and non-random planar sets. We also analyse stability of β-skeletons and their sensitivity to perturbations.

© 2013 Elsevier Inc. All rights reserved.

1. Introduction

A planar graph consists of nodes which are points of Euclidean plane and edges which are straight segments connecting the points. A planar proximity graph is a planar graph where two points are connected by an edge if they are close in some sense. Usually a pair of points is assigned certain neighbourhood, and points of the pair are connected by an edge if their neighbourhood is empty. Delaunay triangulation [10], relative neighbourhood graph [12] and Gabriel graph [18], and indeed spanning tree, are most known examples of proximity graphs.

β-skeletons [14] is a unique family of proximity graphs monotonously parameterised by β. Two neighbouring points of a planar set are connected by an edge in β-skeleton if a lune-shaped domain between the points contains no other points of the planar set. Size and shape of the lune is governed by β.

Why is it necessary to study properties of β-skeletons? The β-skeletons are eminent representatives of the family of proximity graphs. Proximity graphs found their applications in fields of science and engineerings: image processing and computational morphology: e.g. curve reconstruction from a set of planar points [4], approximation of road networks [27,28], geographical variational analysis [11,18,22], evolutionary biology [17], spatial analysis in biology [15,8,9,13], simulation of epidemics [25]. Proximity graphs are used in physics to study percolation [6] and analysis of magnetic field [24]. Engineering applications of proximity graphs are in message routing in ad hoc wireless networks, see e.g. [16,23,21,19,26], and visualisation [20]. Road network analysis is yet another field where proximity graphs are invaluable. Road networks are well matched by relative neighbourhood graphs, see e.g. study of Tsukuba central district [27,28]. Biological transport networks also bear remarkable similarity to certain proximity graphs. Foraging trails of ants and protoplasmic networks of slime mould *Physarum polycephalum* [1,2] are most striking examples.

In our previous works on approximation of man-made road networks with slime mould and proximity graphs [2] we found that β-skeletons provides sufficiently good approximation of highway network in many countries for β lying between 1 and 2 (Fig. 1a and b). A β-skeleton, in general case, becomes disconnected for β > 2 and continues losing its edges with further increase of β (Fig. 1c–l). Are sections of road networks, which survive longer with increasing β bear any particular

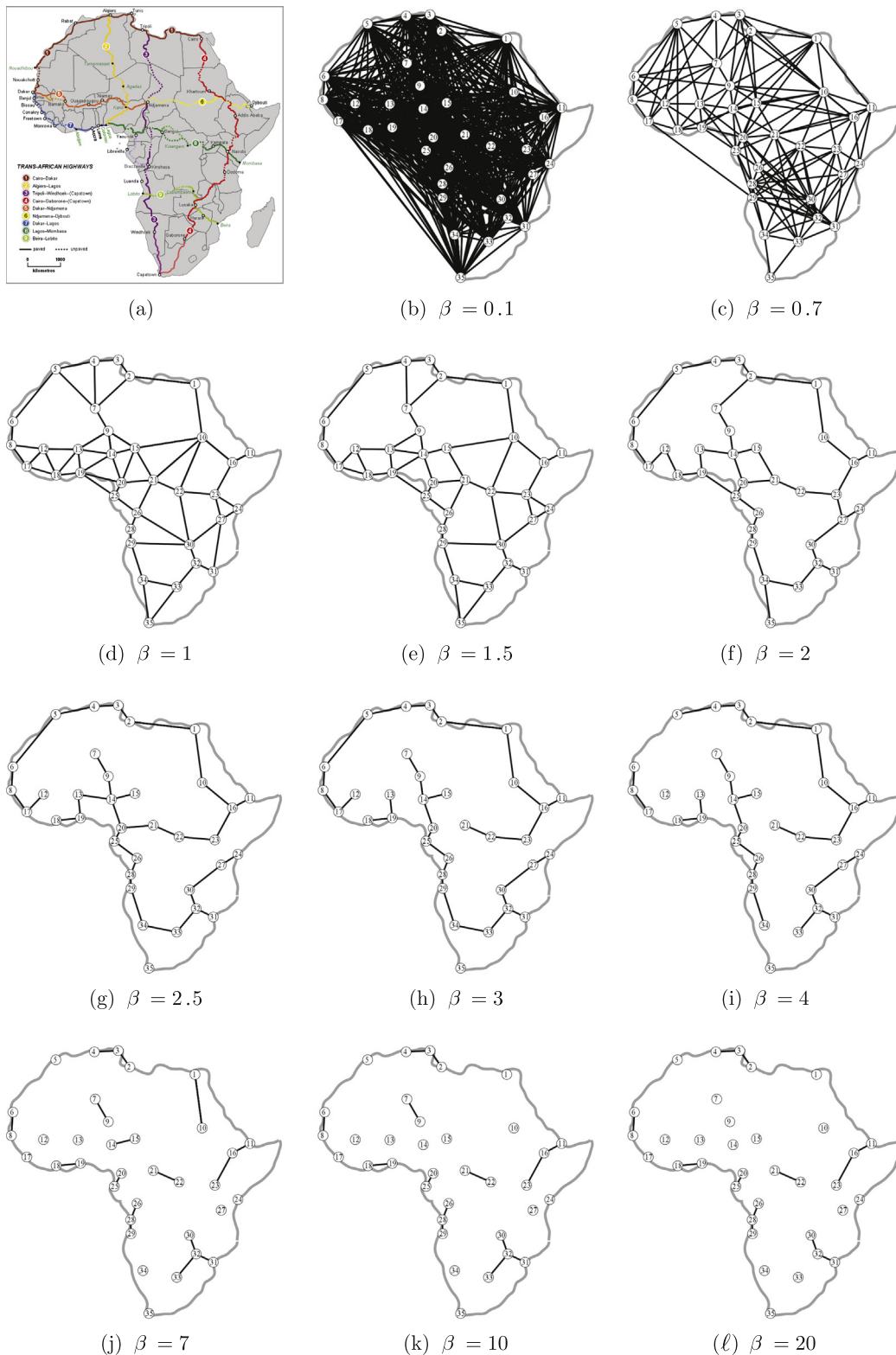*E-mail address:* andrew.adamatzky@uwe.ac.uk

(a)   (b) $\beta = 0.1$ (c) $\beta = 0.7$

(d) $\beta = 1$ (e) $\beta = 1.5$ (f) $\beta = 2$

(g) $\beta = 2.5$ (h) $\beta = 3$ (i) $\beta = 4$

(j) $\beta = 7$ (k) $\beta = 10$ (ℓ) $\beta = 20$

Fig. 1. β-skeleton approximation of African highways. (a) original scheme of trans-African highways [29]. (b)–(l) β-skeletons on major urban areas are illustrated for selected values of β from 0.1 to 20. See details in [2,3].

55 importance? We did find, see details in [2,3], that by tuning value of β we can, in principle, make a difference between paved
56 and unpaved roads in Trans-African highway network, however an ideal matching between a β-skeleton and a high-way
57 graph was every achieved. Thus we got engaged with studies of dynamics of β-skeletons. Some finding we made so far
58 are outlined in present paper. We answer the following questions. How a rate of edge disappearance depends on β? For what
59 configurations of planar points β-skeleton does not lose its edges with increase of β? Can we differentiate between random
60 and non-random configurations of planar points by a curve of their β-driven edge disappearance?

2. β-Skeletons

62 Given a set **V** of planar points, for any two points p and q we define β-neighbourhood $U_\beta(p,q)$ as an intersection of two
63 discs with radius $\beta|p - q|/2$ centred at points $((1 - \frac{\beta}{2})p, \frac{\beta}{2}q)$ and $(\frac{\beta}{2}p, (1 - \frac{\beta}{2})q), \beta \geqslant 1$ [14,12], see examples of the lunes in
64 Fig. 2. Points p and q are connected by an edge in β-skeleton if the pair's β-neighbourhood contains no other points from **V**.
65 A β-skeleton is a graph $G_\beta(\mathbf{V}) = \langle \mathbf{V}, \mathbf{E}, \beta \rangle$, where nodes $\mathbf{V} \subset \mathbf{R}^2$, edges **E**, and for $p, q \in \mathbf{V}$ edge $(pq) \in \mathbf{E}$ if $U_\beta(p,q) \cap \mathbf{V}/\{p,q\} = \emptyset$.
66 Parameterisation β is monotonous: if $\beta_1 > \beta_2$ then $G_{\beta_1}(\mathbf{V}) \subset G_{\beta_2}(\mathbf{V})$ [14,12]. A β-skeleton is Gabriel graph [18] for $\beta = 1$ and the
67 skeleton is relative neighbourhood graph for $\beta = 2$ [14,12].

3. Edges losses in skeleton on random planar sets

69 To analyse rate of edge losses in β-skeletons of random planar sets we represented planar points by n discs, centres of the
70 discs form set **V**. Each disc has a radius 2.5 units and the discs are randomly distributed in a large disc with radius 250
71 (Fig. 3). For n up to 2500 and β varying from 1 to 50 we calculated number of edges $e(n,\beta)$ in β-skeletons (Fig. 3b–h). Example
72 curves are shown in Fig. 3i. Data points $e(n,\beta)$ are approximated by power curve $e(n,\beta) \sim c(n,\beta) \cdot \beta^{\alpha(n,\beta)}$.

73 **Finding 1.** β-skeletons of random planar sets lose their edges by power law. Number decreases proportionally to β^α, $\alpha < 0$.
74 Absolute value of α is linearly proportional to number of planar points in the sets.
75 To uncover how $c(n,\beta)$ and $\alpha(n,\beta)$ depends on n we approximated $e(n,\beta)$ for planar sets $n = 50, 60, 70, \ldots, 2500$ and $\beta = 1$,
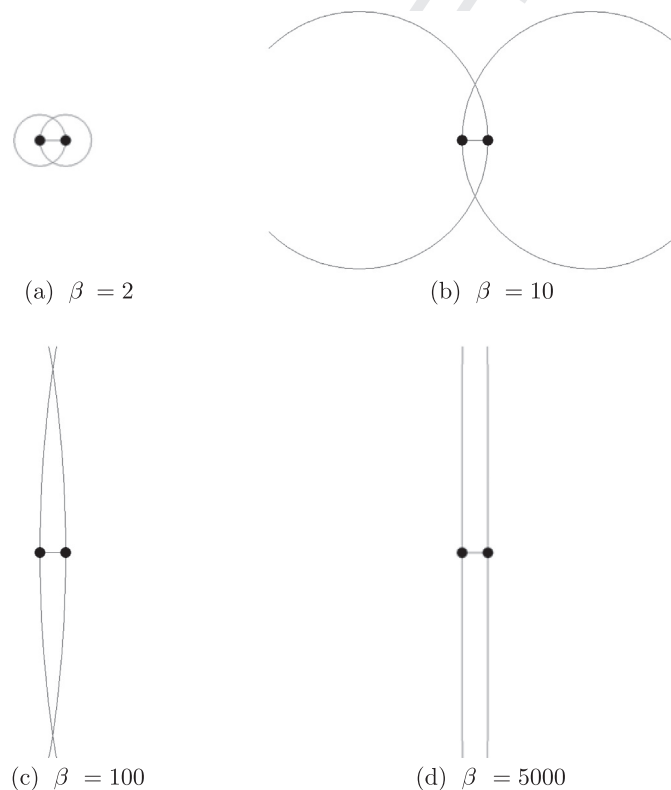76 2, 3, $\ldots$, 50. Data points calculated are shown in Fig. 4.

(a) $\beta = 2$ (b) $\beta = 10$

(c) $\beta = 100$ (d) $\beta = 5000$

Fig. 2. Examples of lunes (β-neighbourhoods) of two planar points (small circles) for various values of β.

(a) **V**   (b) $\beta = 1$ (c) $\beta = 2$

(d) $\beta = 7$ (e) $\beta = 10$ (f) $\beta = 100$
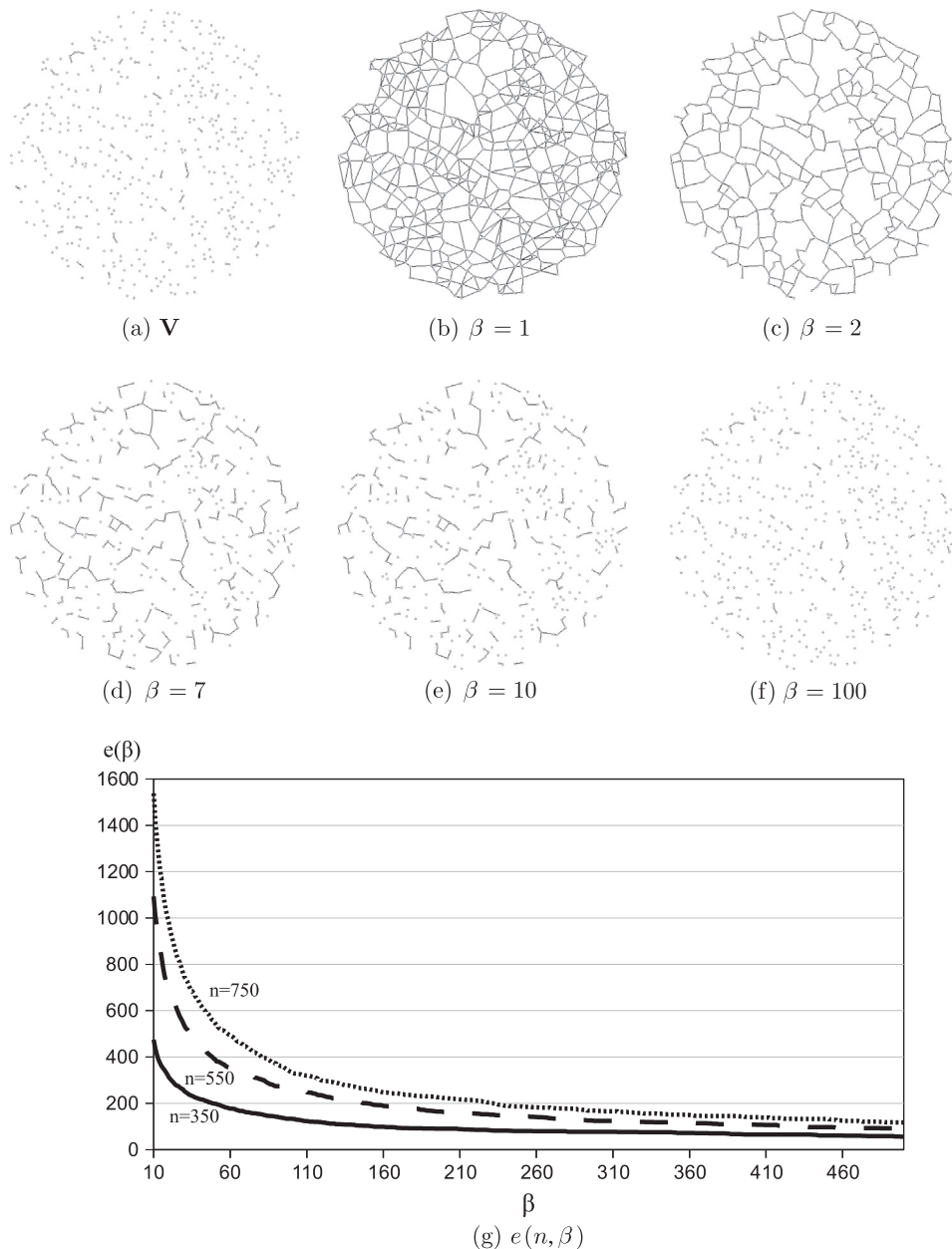
(g) $e(n, \beta)$

Fig. 3. Skeletons of a random planar set **V** (a) lose their edges with increase of β. (b–h) Examples of *beta*-skeletons on planar set of 500 discs, radius 2.5 each, randomly distributed in a disc radius 250. (i) Example power curves $e(n, \beta)$, $1 \leqslant \beta \leqslant 50$, $n = 350$ (solid line), $n = 550$ (dashed line) and $n = 750$ (fine dashed line), values of β are incremented by 0.1.

77   Coefficient $\alpha(n, \beta)$ linearly decreases (increases in its negative values) with increase of a number of nodes (Fig. 4a). Coef-
78 ficient $c(n, \beta)$ increases proportionally to β^b for $n \leqslant 700$ (Fig. 4b) and the coefficient grows proportionally to d^β for $n > 700$
79 (Fig. 4c), where $1 \leqslant b, d \leqslant 2$.

80   **4. Differentiating between random and non-random sets**

81   In previous section we demonstrated that presence of even minor impurities in originally regular arrangement of planar
82 points can be detected directly in the shape of edge disappearance curve $e(n, \beta)$. This leads us to the following hypothesis.

83   **Hypothesis 1.** Random planar sets can be differentiated from non-random sets by a shape of edge disappearance curve
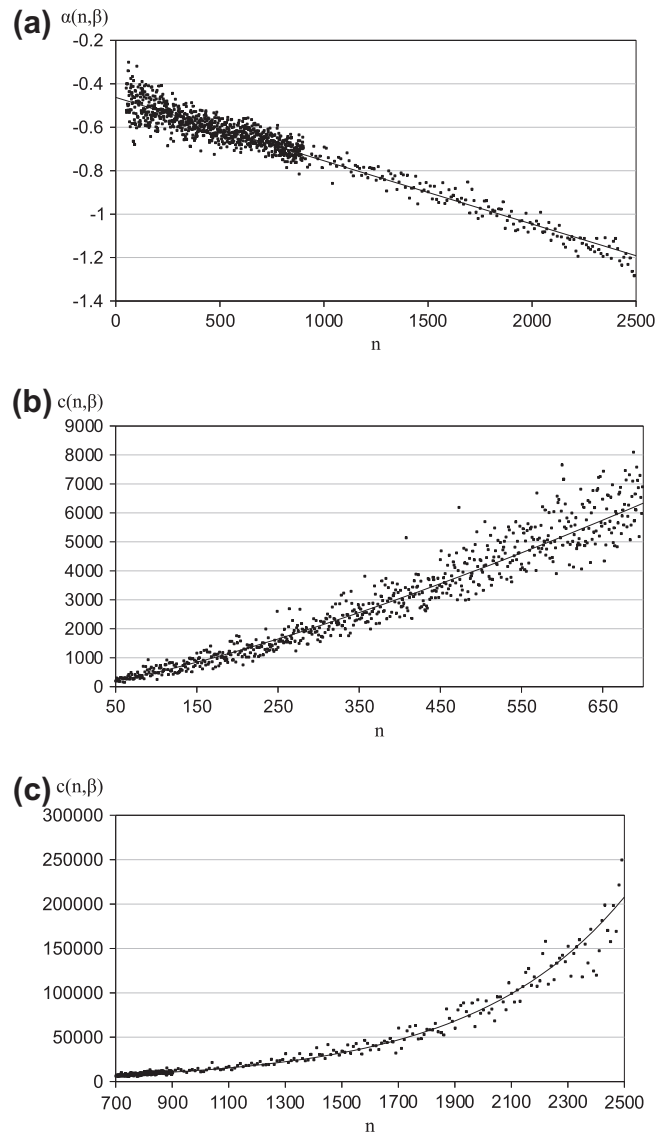84 $e(n, \beta)$.

Fig. 4. Approximation of coefficients $c(n,\beta)$ and $\alpha(n,\beta)$ of $e(n,\beta) = c(n,\beta) \cdot n^{\alpha(n,\beta)}$ for n up to 2500: (a) $\alpha(n,\beta)$, linear approximation line $\alpha(n,\beta) = -0.0003\beta \cdot 0.4628$, $R = 0.925$; (b) $c(n,\beta)$, $50 \leqslant n \leqslant 700$, $c(n,\beta) = 1.2072 \cdot \beta^{1.3075}$, $R = 0.957$; (c) $c(n,\beta)$, $700 \leqslant n \leqslant 2500$, $c(n,\beta) = 1998.5 \cdot 1.0019^{\beta}$.

We do not aim to prove the hypothesis in present paper but rather demonstrate its viability in two examples. We represented drawings of a face and a horseman and in sets of planar points (Figs. 5a and 6a). Evolution of β-skeletons of these sets, associated with removal of certain edges of β-skeletons, leads to formation of contour like representations of the images (Figs. 5 and 6). We calculated edge disappearance curves $e(n,\beta)$ for fixed n and β changing from 1.0 to 50 with increment 0.1 (Fig. 7, dashed line and dash-dots line). We also produced curves $e(n,\beta)$ for random sets of planar points, with the same numbers of points, distributed in a disc radius 250 units (Fig. 7, solid line and dotted line).

The data are approximated by power regression $c(n,\beta) \cdot \beta^{\alpha(n,\beta)}$ with coefficients shown in Table 1. The coefficients were calculated using a non-linear least square technique using Gauss–Newton algorithm [7].

Based on Fig. 7 and Table 1 we can conclude that random planar sets have initially higher number of edges than non-random sets however they exhibit higher rate of edge disappearance driven by β. For $\beta = 1$ a number of edges in the skeleton of face is 0.72 of edges comparing to ta number of edges in a skeleton of a random planar set with the same number of points; and skeleton of horseman has 0.79 of edges of its corresponding random set. The skeletons of non-random sets have almost the same number of edges as skeletons of random sets at $\beta = 2.4$ (face) and $\beta = 2.7$ (horseman). After that value of β number of edges in skeletons of random sets decreases substantially quicker than number of edges of skeletons of non-random sets. Thus, at $\beta = 50$ β-skeleton of face has 4.68 times more edges than a skeleton of its corresponding random set, and skeleton of horseman has 2 times more edges than skeleton of a random set.
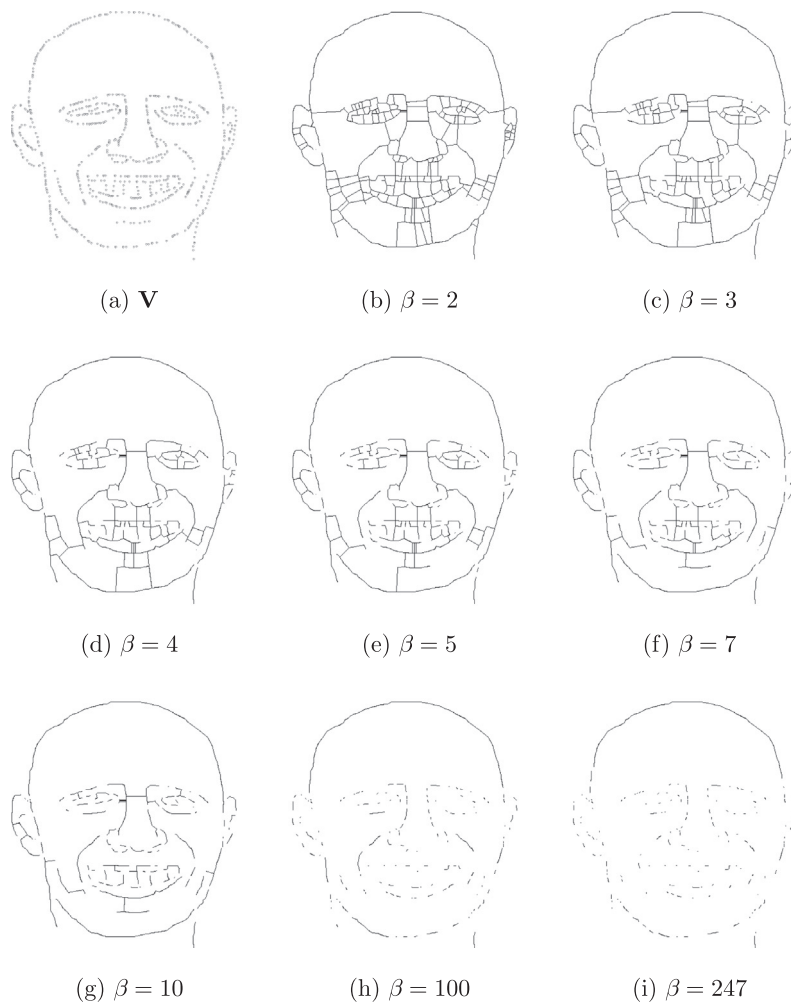
INS 10207
13 August 2013
ARTICLE IN PRESS
No. of Pages 12, Model 3G
Q1 6
A. Adamatzky / Information Sciences xxx (2013) xxx–xxx

Fig. 5. A drawing of a face represented by planar points **V** with $n = 823$ nodes and its β-skeletons for $2 \leqslant \beta \leqslant 247$; $n = 823$.

101 The two examples considered are not at all enough to make any rigorous conclusions, however we can speculate that the
102 difference between random and non-random sets occurs when β is changed from 2 to 3 (i.e. almost at the same time when
103 skeletons are at first becoming disconnected); and, it is enough to compute β-skeletons till $\beta = 10$ because for such value of β
104 number of edges in skeletons of non-random sets 1.5 times higher than a number of edges in skeletons of random sets.

5. Stability and impurities

106 Not all β-skeletons lose their edges with increase of β. Special cases of stable β-skeletons are discussed in present section.
107 Let $\mathbf{B}_{ab}$ be an open half-plane bounded by an infinite straight line l_a passing through a, perpendicular to segment (a,b) and
108 containing b; and $\mathbf{B}_{ba}$ be an open half-plane bounded by an infinite straight line l_b perpendicular to segment (a,b), passing
109 through b and containing a. Let $\mathbf{H}_{ab} = \mathbf{B}_{ab} \cap \mathbf{B}_{ba}$. When β becomes extremely large, tends to infinity, a β-neighbourhood of any
110 two neighbouring points a and b tends to $\mathbf{H}_{ab}$. A β-skeleton of planar set **V** is stable if for any $a,b \in \mathbf{VL}_{ab}$ does not contain any
111 points from **V** apart of a and b. A stable β-skeleton retains its edges for any value of $\beta > 1$.
112 A most obvious example of a stable β-skeleton is a skeleton built on a set of planar points arranged in a rectangular array.
113 The rectangular β-skeleton conserves its edges for any value of β (Fig. 8). The rectangular attice is stable because for any two
114 neighbouring nodes a and b intersection of their half-planes $\mathbf{H}_{ab}$ fits between rows or columns of nodes without covering any
115 nodes.

116 **Finding 2.** Regularity does not guarantee stability.

117 In Fig. 9 we show skeletons of a hexagonal arrangement of planar points (Fig. 9a). A skeleton is a hexagonal lattice for
118 $\beta = 1$ (Fig. 9b). All diagonal edges of the lattice disappear when $\beta = 2$ (Fig. 9c). With further increase of β to 3 horizontal edges
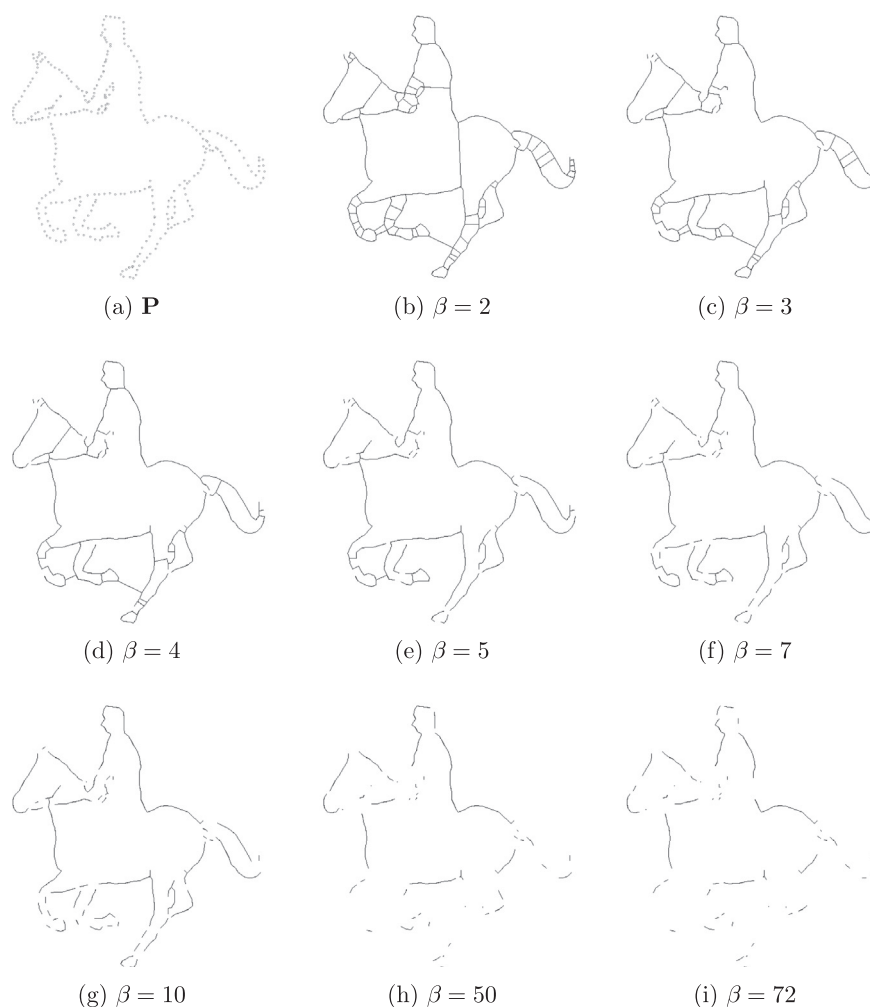119 vanish (Fig. 9d) and all nodes of the original planar set become isolated.

(a) **P**   (b) $\beta = 2$ (c) $\beta = 3$

(d) $\beta = 4$ (e) $\beta = 5$ (f) $\beta = 7$

(g) $\beta = 10$ (h) $\beta = 50$ (i) $\beta = 72$

Fig. 6. A drawing of a horseman represented by planar points **V** with $n = 351$ nodes and the β-skeletons of **V** for selected values of $2 \leqslant \beta \leqslant 72$.
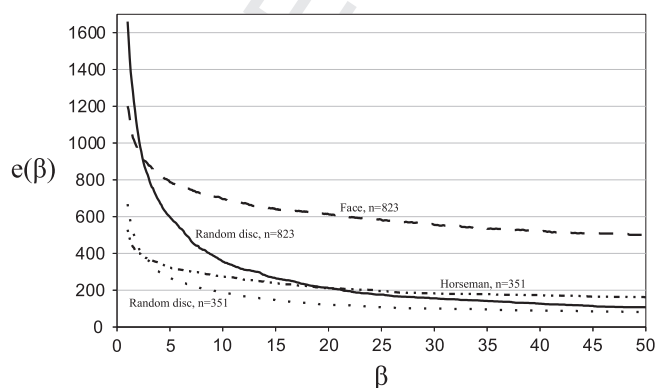

Fig. 7. Edge disappearance curves $e(n, \beta)$ of β-skeletons constructed over planar points representing face (Fig. 5), shown by dashed line; horseman (Fig. 6), shown by line of dashes and dots; and two random set of planar points, distributed in discs, with the same number of points as face and horseman, shown by solid and dotted lines, respectively. Values of β are incremented by 0.1.

Finding 3. Stable β-skeletons are sensitive to perturbations.

Stable β-skeletons are sensitive to even slight distortions of a regular arrangement of elements **V**. This is illustrated in Fig. 10. One node in the otherwise perfect uniform and regular rectangular array of planar points (Fig. 10a) gets its coordinates slightly randomised, so its x coordinate is different from other nodes in its row, and its y coordinate is different from

Table 1
Coefficients of power regression approximation $c(n,\beta) \cdot \beta^{\alpha(n,\beta)}$ of β-driven edge disappearing in β-skeletons of non-random and random planar sets.

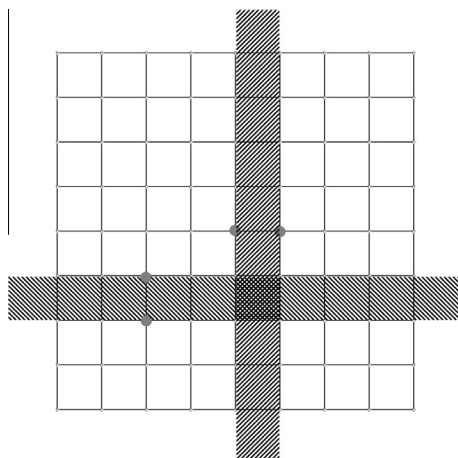| Planar set	n	$c(n,\beta)$	$\alpha(n,\beta)$
Face	823	1797.9	−0.296
Random set	823	10078.9	−0.73
Horseman	351	1077.8	−0.306
Random set	351	2159.0	−0.5344

Fig. 8. Rectangular lattice is a stable β-skeleton. β-neighbourhoods, $\beta \to \infty$, of two pairs of nodes (marked by large discs) are shown by hatched areas.
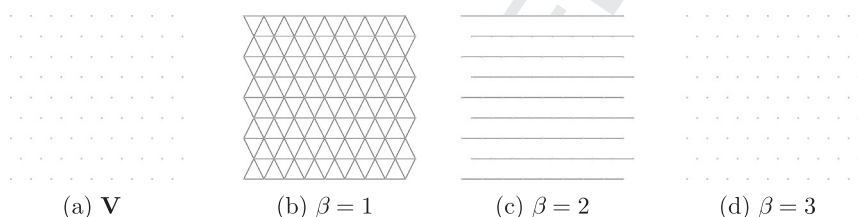

(a) **V**   (b) $\beta = 1$ (c) $\beta = 2$ (d) $\beta = 3$

Fig. 9. Transformation of β-skeletons built on a hexagonal array of planar points **V**.

(a) **V**   (b) $\beta = 2$ (c) $\beta = 10$ (d) $\beta = 11$

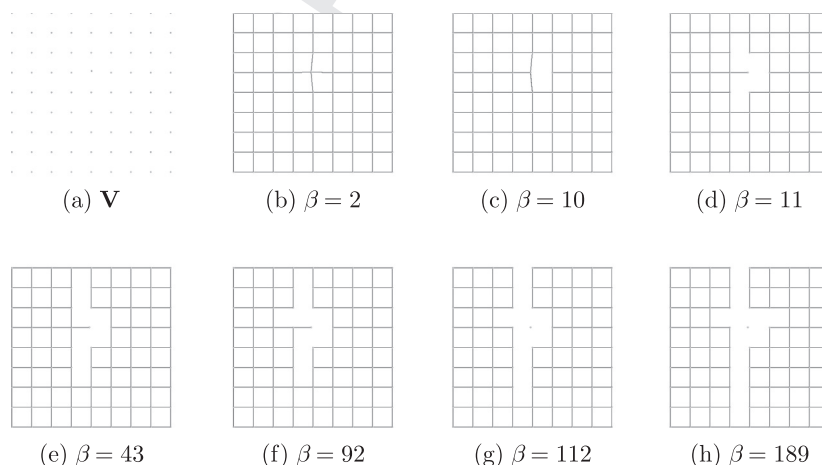(e) $\beta = 43$ (f) $\beta = 92$ (g) $\beta = 112$ (h) $\beta = 189$

Fig. 10. Transformation of β-skeleton on planar points arranged in a rectangular array (a) with a single 'defective' node in 5th column and 4th row.
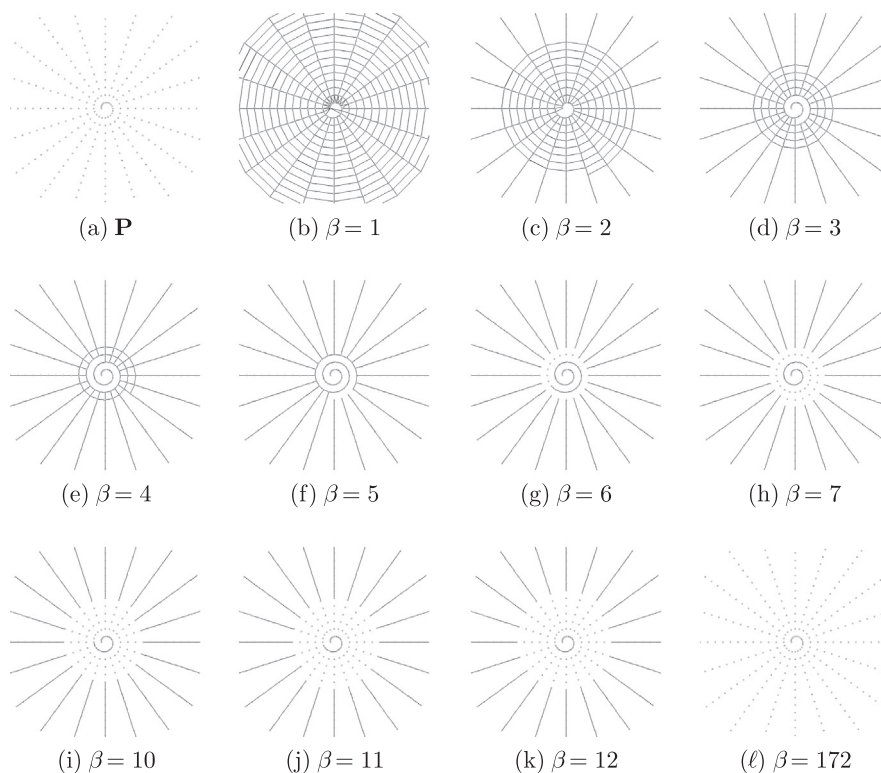
(a) **P**   (b) $\beta = 1$ (c) $\beta = 2$ (d) $\beta = 3$

(e) $\beta = 4$ (f) $\beta = 5$ (g) $\beta = 6$ (h) $\beta = 7$

(i) $\beta = 10$ (j) $\beta = 11$ (k) $\beta = 12$ (ℓ) $\beta = 172$

Fig. 11. Restructuring of a spider-web β-skeleton by increasing β.

other nodes in its column. A localised distortion of the skeleton can be seen in edges linking node in 5th column and 4th row with its four neighbours (Fig. 10b). With increase of β the 'defective' node starts losing its edges (Fig. 10c). With further increase of β the defect induced edge elimination propagates along row and columns adjacent to the defective node (Fig. 10d–g). Eventually a value of β reached where no more edges are removed and the skeleton remains stable under subsequent growth of β (Fig. 10h).

When regular β-skeletons are 'dissolved' by increasing β order of an edge disappearance is determined by the edge location. In Fig. 11a we consider a planar set which core nodes are arranged in a spiral and other nodes lined up in rays. The planar set is spanned by spider-web looking β-skeleton for $\beta = 1$ (Fig. 11b). The spiral part of the skeleton retracts back towards its centre when β increases from 1 to 4 (Fig. 11cde). At the value $\beta = 5$ only nodes which where originally in the spiral shape (two rotations) and nodes aligned in rays are connected by edges of the β-skeleton (Fig. 11f). Further increase of β causes retraction of the original spiral and dilution of rays, with edges disappearing centrifugally (Fig. 11g–l).

Finding 4. Presence of impurities in otherwise regular arrangements can be detected by edge disappearance curve $e(\beta, n)$.

Let us consider a planar set where points are arranged into six nested circles all centred at the same point c (Fig. 12a). When $\beta = 1$ the skeleton has the following structure: every point in circle A is connected by an edge to its two immediate neighbours in its circle, and to two neighbours in the circle included in A (if there is a circle included in A) and two neighbours in the circle which includes A (if there is a circle including A), see Fig. 12b. Increase of β from 1 to 11 leads to disappearance of edges connecting points in different circles (Fig. 12c–k). These edges disappear centrifugally. With further increase of $\beta > 11$ we observe removal of edges linking nodes in the same circles, see e.g. (Fig. 12c–k).

Let us introduce a minor impurity: we make centres of circles slightly deviating, at random in a range $[-5,5]$ units along each axis, around centre c (Fig. 13a). With increase of β the skeleton of such an arrangement of points loses majority of edges between different circles when β reaches 7 (Fig. 13b–g). Few remaining edges are removed by $\beta = 11$ (Fig. 13h–k). Edges connecting points inside circles disappear for larger values of β, see e.g. (Fig. 13l).

Edge disappearance curves $e(n, \beta), n = 241$, for the β-skeletons of the cyclic arrangements are shown in Fig. 14. For comparison we also added $e(n, \beta)$ for six nested circles with the same centre c where position of each point is randomised in interval $[-2,2]$ along each axis.

The curve $e(n, \beta)$ for circular arrangement of points with the same centre has a pronounced staircase like structure (Fig. 14, solid line). The first sequence of low-height stairs is observed for $1 \leqslant \beta \leqslant 1.5$: this corresponds to removal of edges connecting points lying in different cycles. The second sequence of stairs, $2 \leqslant \beta \leqslant 5$ reflects removal of edges linking neighbouring
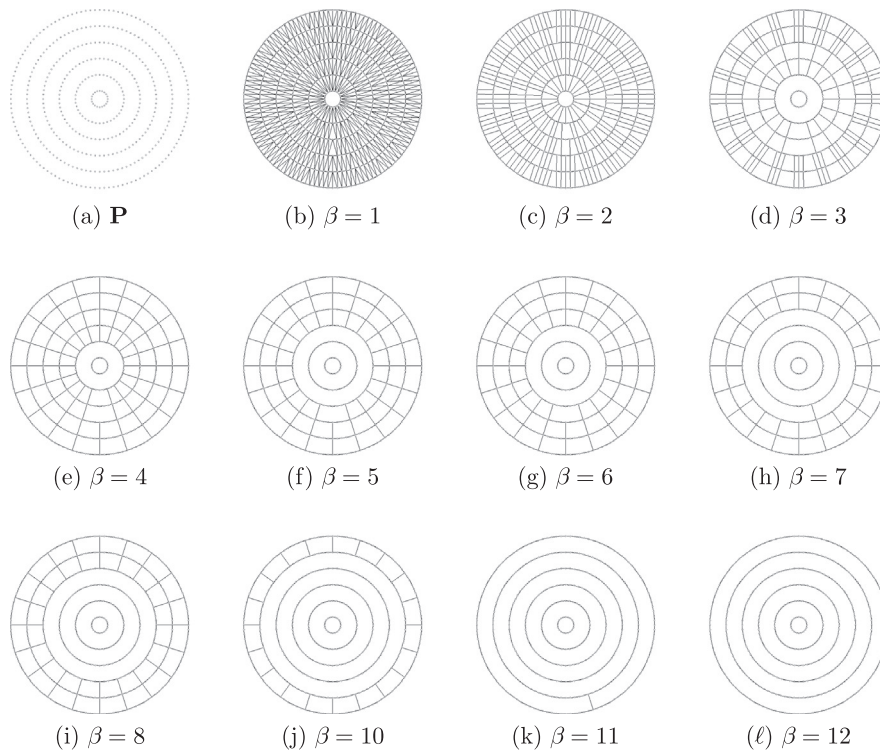
INS 10207
13 August 2013

ARTICLE IN PRESS

No. of Pages 12, Model 3G

Q1 10

A. Adamatzky / Information Sciences xxx (2013) xxx–xxx

(a) **P**   (b) $\beta = 1$ (c) $\beta = 2$ (d) $\beta = 3$

(e) $\beta = 4$ (f) $\beta = 5$ (g) $\beta = 6$ (h) $\beta = 7$

(i) $\beta = 8$ (j) $\beta = 10$ (k) $\beta = 11$ (ℓ) $\beta = 12$

Fig. 12. A β-skeletons of planar points arranged in six nested circles centred at the same point *c*.

(a) **P**   (b) $\beta = 1$ (c) $\beta = 2$ (d) $\beta = 3$

(e) $\beta = 4$ (f) $\beta = 6$ (g) $\beta = 7$ (h) $\beta = 8$

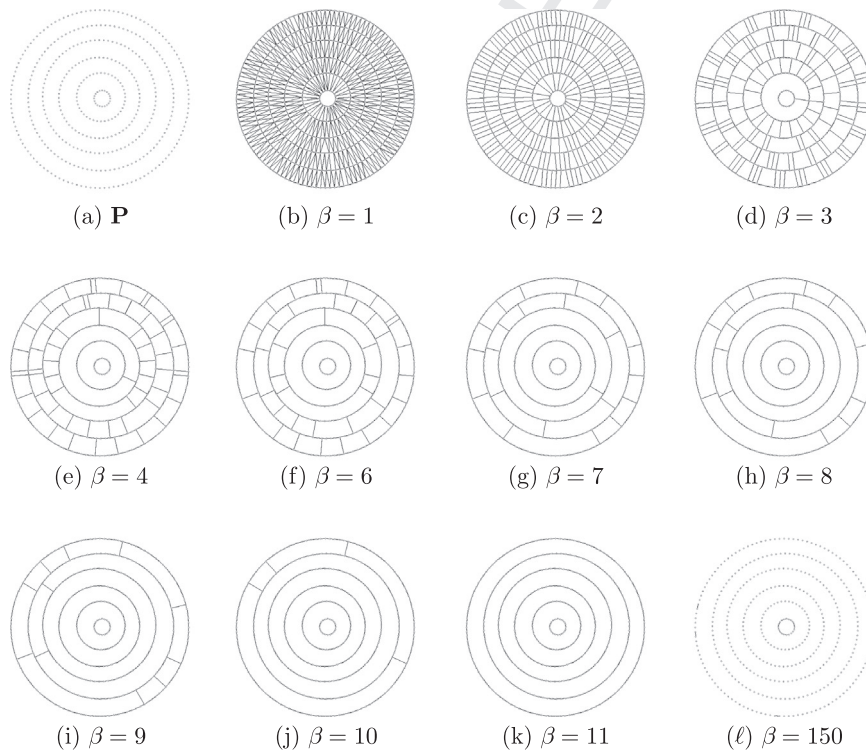(i) $\beta = 9$ (j) $\beta = 10$ (k) $\beta = 11$ (ℓ) $\beta = 150$

Fig. 13. β-skeletons of planar points arranged in six nested circles centred with minor, $[-5,5]$ units, random deviations from original point *c* (*c* is used as centre in Fig. 12).
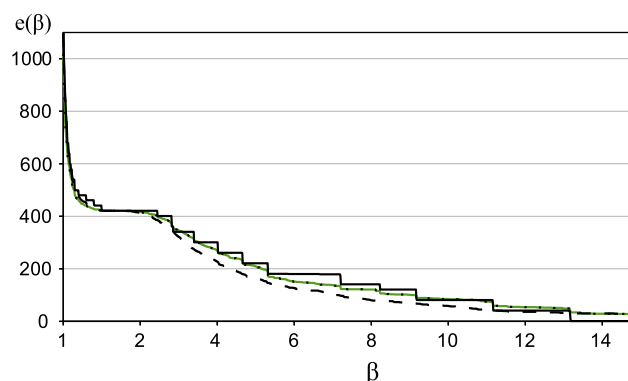
Fig. 14. Edge disappearance curves $e(n, \beta)$ of β-skeletons constructed over planar points arranged in (solid line) six nested circles with the same centre c (as Fig. 12), (dashed line) six nested circles with centres slightly randomly deviated from c (Fig. 13) grey line with black dots) six nested circles with the same centre c yet positions of points randomised in interval $[-2,2]$ along each axis; $n = 241$, values of β are incremented by 0.1.

points lying in the same cycles. Curves $e(n, \beta)$, calculated for circular arrangement of points with randomised centres and circles with randomised positions of nodes, show gradual decline in number of edges.

6. Conclusion

Most β-skeletons lose their edges with increase of β. The skeletons of random planar sets lose edges by power low with rate of edge disappearance proportional to a number of points in the sets. Some β-skeletons conserve their edges for any β as large as it could be. These are usually skeletons built on a regularly arranged points of planar sets. We found that even minuscule impurity in the regular arrangement of points leads to propagation of edge loss wave across the otherwise stable skeleton. This indicates that presence of random components in a planar set may lead to a higher rate of β-driven edge disappearance. By comparing edge disappearance curves of non-random and random planar sets (with the same number of nodes) we found that β-skeletons of random sets have larger number of edges for small values of β (up to $\beta = 2.5$–3) yet exhibit higher rate of edge loss. In examples studied skeletons of random sets lose their edges 1.5–2.5 times faster than skeletons of non-random set. For large values of β ($\beta > 25$) a number of edges in β-skeletons of non-random planar sets is over twice a number of edges in random sets. We hypothesise that by subjecting a β-skeleton of a planar set to β-driven edge removal we can discriminate between random and non-random sets. To prove the hypothesis and make the approach applicable to image classification we must collect statistics form much larger number of non-random planar sets. This will be a topic of further studies.

7. Uncited reference

Q2   [5].

References

[1] A. Adamatzky, Developing proximity graphs by *Physarum polycephalum*: Does the plasmodium follow Toussaint hierarchy?, Parallel Processing Letters 19 (2008) 105–127
[2] A. Adamatzky (Ed.), Bioevaluation of World Transport Networks, World Scientific, 2012.
[3] A. Adamatzky, A. Kayem, Biological evaluation of trans-African highways, The European Physical Journal Special Topics 215 (1) (2013) 49–59.
[4] N. Amenta, M. Bern, D. Eppstein, The crust and the β-skeleton: combinatorial curve reconstruction, Graphical Models and Image Processing 60 (1998) 125–135.
[5] D.J.K. Beavon, P.L. Brantingham, P.J. Brantingham, The Influence of Street Networks on the Patterning of Property Offenses. <http://www.popcenter.org/library/CrimePrevention/Volume_02/06beavon.pdf>.
[6] J.M. Billiot, F. Corset, E. Fontenas, Continuum percolation in the relative neighbourhood graph. arXiv:1004.5292.
[7] A. Björck, Numerical Methods for Least Squares Problems, SIAM, 1996.
[8] M.R.T. Dale, Spatial Analysis in Plant Ecology, Cambridge University Press, 2000.
[9] M.R.T. Dale, P. Dixon, M.-J. Fortin, P. Legendre, D.E. Myers, M. S Rosenberg, Conceptual and mathematical relationships among methods for spatial analysis, Ecography 25 (2002) 558–577.
[10] B. Delaunay. Sur la sphère vide, Izvestia Akademii Nauk SSSR, Otdelenie Matematicheskikh i Estestvennykh Nauk 7 (1934) 793–800.
[11] K.R. Gabriel, R.R. Sokal, A new statistical approach to geographic variation analysis, Systematic Zoology 18 (1969) 259–270.
[12] J.W. Jaromczyk, G.T. Toussaint, Relative neighborhood graphs and their relatives, Proc. IEEE 80 (1992) 1502–1517.
[13] T. Jombart, S. Devillard, A.-B. Dufour, D. Pontier, Revelaing cryptic spatial patterns in genetic variability by a new multivariate method, Heredity 101 (2008) 92–103.
[14] D.G. Kirkpatrick, J.D. Radke, A framework for computational morphology, in: G.T. Toussaint (Ed.), Computational Geometry, North-Holland, 1985, pp. 217–248.
[15] P. Legendre, M.-J. Fortin, Spatial pattern and ecological analysis, Vegetatio 80 (1989) 107–138.

INS 10207
13 August 2013

ARTICLE IN PRESS

No. of Pages 12, Model 3G

Q1 12

A. Adamatzky / Information Sciences xxx (2013) xxx–xxx

[16] X.-Y. Li, Application of computation geometry in wireless networks, in: X. Cheng, X. Huang, D.-Z. Du (Eds.), Ad Hoc Wireless Networking, Kluwer Academic Publishers, 2004, pp. 197–264.

[17] P.W. Magwene, Using correlation proximity graphs to study phenotypic integration, Evolutionary Biology 35 (2008) 191–198.

[18] D.W. Matula, R.R. Sokal, Properties of gabriel graphs relevant to geographic variation research and clustering of points in the plane, Geographical Analysis 12 (1980) 205–222.

[19] R.B. Muhammad, A distributed graph algorithm for geometric routing in ad hoc wireless networks, Journal of Networks 2 (2007) 49–57.

[20] A. Runions, M. Fuhrer, B. Lane, P. Federl, A.-G. Rolland-Lagan, P. Prusinkiewicz, Modeling and visualization of leaf venation patterns, ACM Transactions on Graphics 24 (2005) 702–711.

[21] P. Santi, Topology Control in Wireless Ad Hoc and Sensor Networks, Wiley, 2005.

[22] R.R. Sokal, N.L. Oden, Spatial autocorrelation in biology: 1. Methodology, Biological Journal of the Linnean Society 10 (2008) 199–228.

[23] W.-Z. Song, Y. Wang, X.-Y. Li, Localized algorithms for energy efficient topology in wireless ad hoc networks, In: Proc. MobiHoc 2004 (May 24–26, 2004, Japan, Roppongi).

[24] M. Sridharan, A.M.S. Ramasamy, Gabriel graph of geomagnetic Sq variations, Acta Geophysica (2010), http://dx.doi.org/10.2478/s11600-010-0004-y.

[25] Z. Toroczkai, H. Guclu, Proximity networks and epidemics, Physica A 378 (2007) 68. arXiv:physics/0701255v1.

[26] P.-J. Wan, C.-W. Yi, On the longest edge of Gabriel Graphs in wireless ad hoc networks, IEEE Transactions on Parallel and Distributed Systems 18 (2007) 111–125.

[27] D. Watanabe, A study on analyzing the road network pattern using proximity graphs, Journal of the City Planning Institute of Japan 40 (2005) 133–138.

[28] D. Watanabe, Evaluating the configuration and the travel efficiency on proximity graphs as transportation networks, Forma 23 (2008) 81–87.

[29] R. Parry, Map of Trans-African Highways based on data 2000 to 2003 (17 July 2007). <http://upload.wikimedia.org/wikipedia/commons/0/03/Map_of_Trans-African_Highways.PNG>.